nzsee
NEW ZEALAND SOCIETY FOR EARTHQUAKE ENGINEERING

Cyclic tests of an innovative seismic bracing member – multiple U-shaped flexural plates dissipater

Y. Chen & A. Palermo
Department of Civil and Natural Resources Engineering, University of Canterbury, Christchurch.

M. Mashal
Department of Civil and Environmental Engineering, Idaho State University, Pocatello, United States

ABSTRACT

Following Canterbury earthquake sequence, there has been an increasing interest in development of low-damage structural design using supplemental damping such as the use of metallic dissipaters. In this research, an innovative seismic bracing member called multiple U-shaped flexural plates (UFP) dissipater (MUD) is proposed. It consists of two rows of UFPs bolted to an internal member and inserted inside a casing. The internal and external members move relative to each other under axial compression and tension loading. Energy dissipation comes from plastic deformation (rolling deformation) of the UFPs. A series of quasi-static cyclic tests were conducted with different arrangements of UFPs and various loading sequences. The mechanical properties, hysteretic characteristics and strength degradation of MUD were investigated. All specimens completed the cycles of displacement corresponding to a 2.8% story drift ratio. The dissipater exhibited stable force-displacement hysteresis and high energy dissipation capacity. Specimen 1, 2 and 3 have been through 28 loading cycles without significant degradation of strength. Specimen 4 has been through three times the maximum credible earthquakes and 46 loading cycles at 2% inter-storey drift ratio (corresponding to a diagonally braced frame with a storey height of 3.0m and a bay length of 3.1m). There was no significant degradation of strength until the last 10 loading cycles where the strength and stiffness started to reduce moderately due to cracking of UFPs.

1 INTRODUCTION

1.1 Background

After the series of Canterbury earthquakes, Christchurch has been suffering serious economic losses due to structural and non-structural damages as well as the downtime. The concept of low-damage and replaceable energy dissipation links is considered in seismic design to achieve better structural performance in major

earthquakes. This means that the building has not only got to satisfy the criteria of life-safe performance level, but also to avoid major structural damage so that the building is operational and economically repairable after major earthquakes (Canterbury Earthquakes Royal Commission., 2012). There are many different types of structural systems which can achieve low-damage/replaceable design, for example, elastic structures, base isolation systems, dissipative rocking systems, Buckling Restrained Brace systems, and supplementary damped structures (Buchanan et al., 2011). In addition, the concept of redundancy design also can be adopted in seismic design. The idea is to design a structure that has more structural components than is necessary. If one structural component is damaged in a major earthquake, the redundant component can be activated and bear the load from the damaged component.

1.2 Metallic damper

Elasto-plastic metallic damper is a type of displacement-activated damper which is able to dissipate energy through plastic deformation of the metal. It can be used in braced structures as a kinetic energy absorbing device. The first research on mechanisms of energy absorption in metallic dampers was conducted by Kelly et al. in the early 1970s. Three mechanisms were investigated, including torsion of square and rectangular steel bars, flexure of short thick steel beams, and rolling of steel strips.

1.3 UFP and MUD

The basic mechanism of U-shaped flexural plates (UFP) is to absorb and dissipate energy through plastic rolling deformation of mild steel. The UFP consists of a semi-circular section (web) with two equal straight sections (flanges) on either side (Figure 1). When the UFP is undergoing rolling motion which causes relative movement between the two flanges, the radius of curvature is changed at the flange-web intersection regions from the initial state to straight in one flange and vice versa in the other flange. Yielding developed in the UFP from the rolling deformation absorbs the kinetic energy generated in the structure by the earthquake (Kelly et al., 1972). UFP dampers have been widely used in the base isolation system in Japan. They exhibited outstanding performance through the 2011 Great East Japan Earthquake (Jiao et al., 2015). There are several applications of the UFPs being used as energy dissipating devices in coupled post-tensioned walls in New Zealand, for example, the Southern Cross Hospital in Christchurch (43°31’13.7”S, 172°38’05.0”E) and the Nelson-Marlborough Institute of Technology in Nelson (43°31’13.7”S, 172°38’05.0”E). Past research on UFPs have shown that they are able to exhibit stable hysteretic behaviour and dissipate energy efficiently. There was no decrease in strength observed during the experimental test.

The Multiple UFPs Dissipater (MUD) is a novel metallic dissipater which has been recently developed by researchers of the University of Canterbury (Mashal et al., 2019). MUD consists of two rows of UFPs been connected to an internal member and an external casing member. The internal member and the external member move relative to each other under axial compression and tension which causes the rolling deformation of the UFPs, hence, energy can be dissipated through the axial movement. The MUD in form of brace type and mini “plug and play” type were conceived and developed by Keats, Palermo and Mashal (2015, 2016). This paper investigates the structural behaviour of the proposed dissipater through large scale experimental testing. The key parameters such as localised damage of UFPs, mechanical properties, hysteretic characteristics and strength degradation are herein shown and some design implications are then drawn at the end of the paper.

2 MATERIALS AND METHODS

2.1 Specimen

The proposed MUD is designed as a structural brace in steel frame to resist earthquake-induced lateral load. The design concept is to achieve the key properties of seismic resilience of structural systems: robustness,

redundancy and rapidity (Bruneau et al., 2003). The specimen consists of two rows of UFPs bolted to an internal member (200 UC 60, Grade 300) and an external casing member (250 x 250 x 9mm SHS, Grade 350L0). The total length of the specimen is 4061mm. Figure 1a and 1b illustrate the shape of the UFP. Dimensions are listed in Table 1. The UFPs were cold-formed, with grade 300L15. One flange of the UFP was bolted to the web of the internal member, the other flange was bolted to the external casing member (Figure 2 and 3). Two M12 bolts (Grade 10.9) were used per flange. All components except for UFPs are designed to remain elastic. They can be reused in each test. When the specimen is subjected to axial load, the internal and external member are moving relative to each other, which causes the rolling deformation of the UFPs (Figure 1c). 17 sets of bolt holes were predrilled on the internal member and the external member so that 17 pairs of UFPs can be installed to reach the full capacity of the member. The redundancy design can be applied in the case that all of the UFPs will be bolted to the web of the internal member but only half of the UFPs will be bolted to the external casing member. After the severe earthquake event the other half of the UFPs will be bolted on and the used UFPs will be released. The MUD device can be relatively easy to repair because it is easy to disassemble. After a major earthquake the used UFPs can be replaced and the device can be reinstalled.

Table 1: Dimensions of UFP

Thickness, t (mm)	Rolled Radius, R (mm)	Length, L (mm)	Height of Flange, H (mm)
10	42.5	160	95

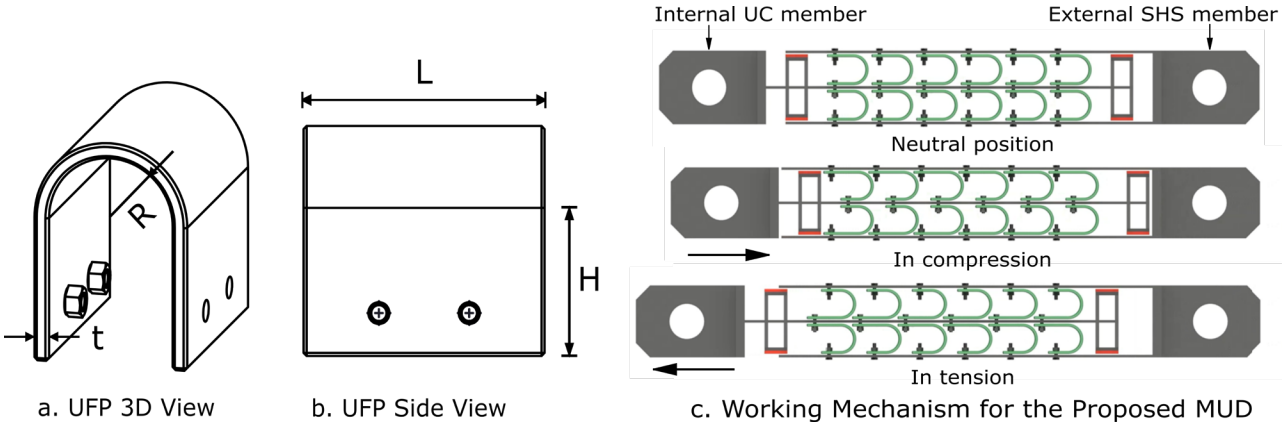

Figure 1: a) UFP 3D view; b) UFP side view; c) Working mechanism for the proposed MUD

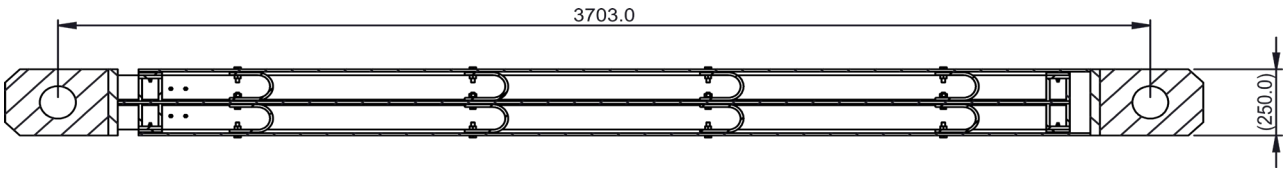

Figure 2: MUD for test 1 and 2, 8 UFPs

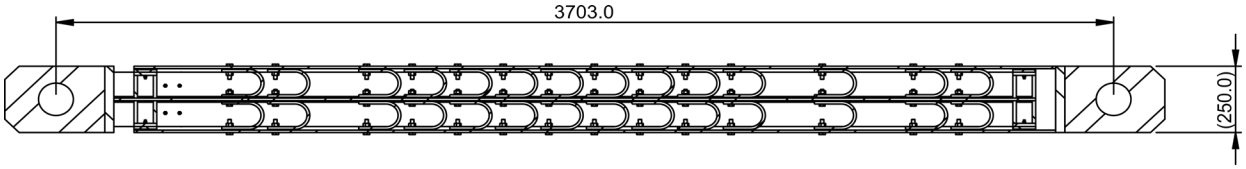

Figure 3: MUD for test 3 and 4, 28 UFPs

2.2 Test setup

Figure 4a shows the test setup. The specimen was tested under axial cyclic loading in the 10MN capacity DARTEC machine in the structural engineering wing lab at University of Canterbury. The specimen was connected to the test machine at the top and bottom by pinned connections.

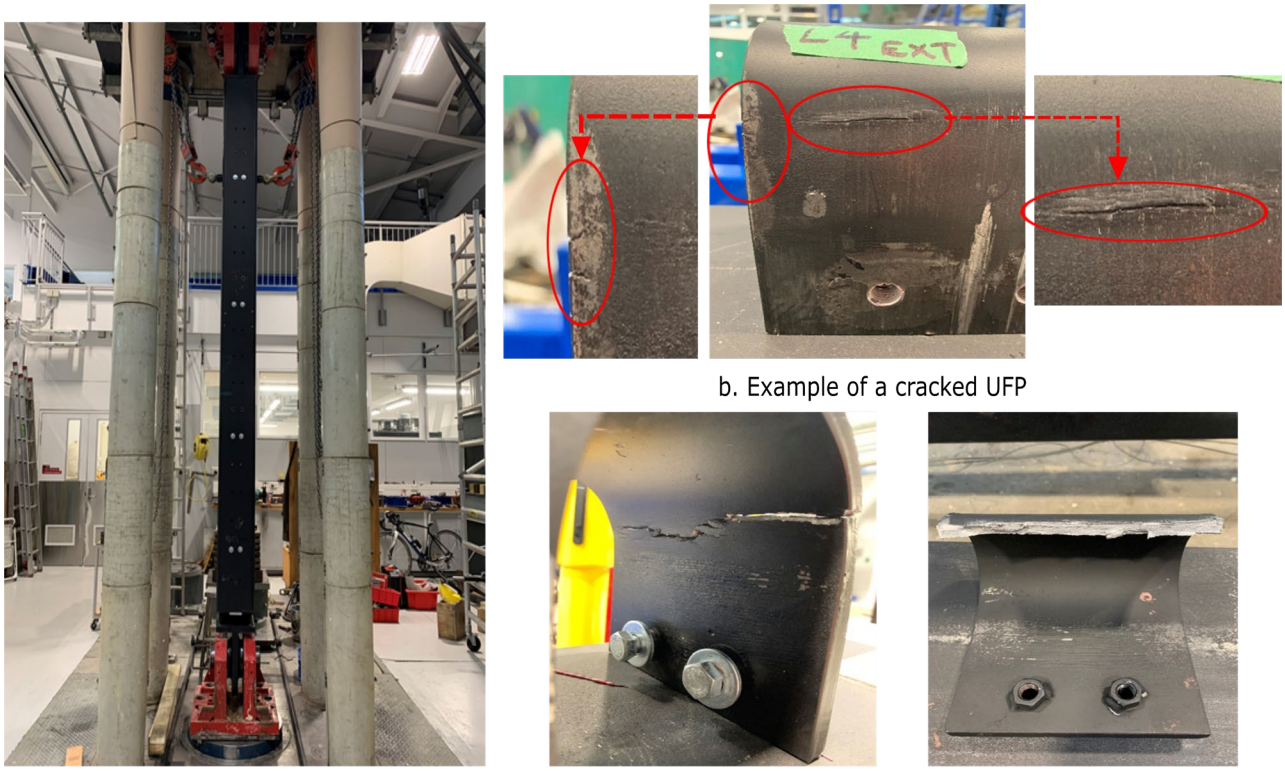

a. Test setup

b. Example of a cracked UFP

c. Example of a fractured UFP

d. Example of a broken UFP

Figure 4: a) Test setup; b) Example of a cracked UFP; c) Example of a fractured UFP; d) Example of a broken UFP

2.3 Test program

Four quasi-static cyclic loading tests were conducted with different arrangements of UFPs and different loading sequences. 8 UFPs were installed in the first two tests (Figure 2). The loading protocol used in the tests was in accordance with AISC 341-16 Seismic Provisions for Steel Building. The design axial displacement (Δ_{bm}) was 30mm, where Δ_{bm} is brace deformation corresponding to the design story drift. The displacement history started from two cycles at the yield deformation (Δ_{by}) of 4mm and followed by two cycles at 0.5, 1.0, 1.5, and 2.0 times the design axial displacement, where the Δ_{by} is the brace deformation at first yield of the test specimen. The specimen was then loaded cyclically at 1.5 times the design axial displacement for 18 cycles. The loading protocol employed a symmetrical triangular displacement-time waveform. The loading rate was 1mm/sec. The AISC 341 – 16 requires that the cumulative inelastic deformation shall be at least 200 times the yield displacement. After the completion of the 2.0 Δ_{bm} cycles, another four cycles at 1.5Δ_{bm} are required to satisfy the requirement, but the proposed loading protocol includes 18 cycles at 1.5 Δ_{bm} which is significantly higher than required to meet the code. In the third and the fourth test, the specimen with 28 UFPs was tested (Figure 3). The same loading history as the first two tests was used for test 3. Different loading history was used in test 4. As illustrated in Figure 5, in phase I (green region) the specimen has met the qualification requirements as specified in AISC 341 – 16. The initial loading sequence was then repeated twice at rate of 4mm/sec (blue region) and 8mm/sec (red region). The specimen was then loaded cyclically at 45mm (1.5Δ_{bm}) for 46 cycles at rate of 2mm/sec, 4mm/sec, 8mm/sec,

12mm/sec and 16mm/sec. The displacement and the axial force of the specimen were recorded by the DARTEC machine.

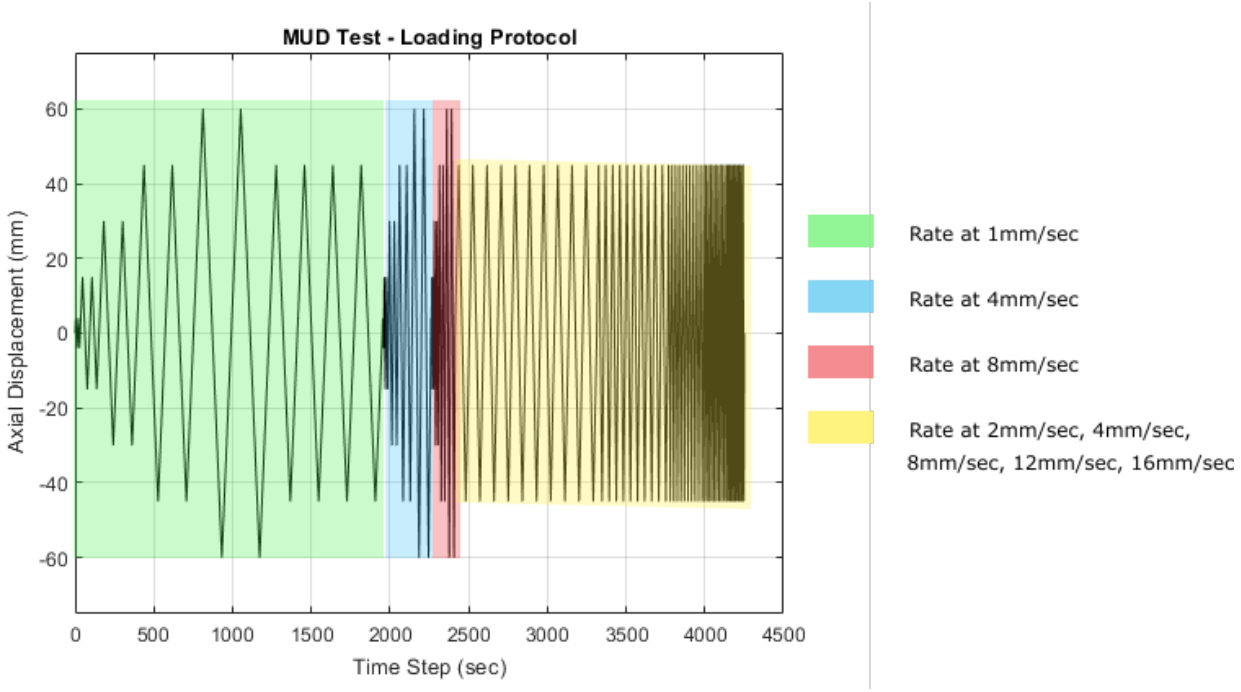

Figure 5: Loading protocol for test 4

3 EXPERIMENTAL RESULTS

3.1 Deformation behaviour

There was no damage observed in the specimen other than the UFPs. Damage of the UFPs were all concentrated at the web-flange intersection region where yielding of the steel occurred through the rolling deformation. There are mainly three types of damage. In order to clarify the difference, the following definitions are made for this report only. Crack in UFP is defined as the surface fissure of the steel plate. Fracture in UFP is the partial separation of the steel plate. Broken UFP means the complete separation of the steel plate. Examples of damage in UFP are shown in Figure 4. The table below summarises the damages of UFPs in each test.

Table 2: Dimensions of UFP

	No. of UFP	No. of Loading Cycles	No. of Cracked UFPs	No. of Fractured UFPs	No. of Broken UFPs
Test 1	8	28	1	0	0
Test 2	8	28	0	1	0
Test 3	28	28	2	0	1
Test 4	28	80	10	8	10

3.2 Results from test 1, 2 and 3

The yield capacity of one UFP can be calculated using the following equation (Baird et al., 2014):

$$F_y = \frac{\sigma_y b_u t_u^2}{2D_u} \quad (1)$$

where σ_y = yield stress of UFP; b_u = width of UFP plate section; t_u = thickness of UFP plate section and D_u = diameter of UFP bend.

Based on the geometry of the UFP, the theoretical yield capacity of a single UFP was 29.5kN. The total yield capacity of 8 UFPs was 236kN. The experimental yield strength ranged from 216.5kN to 265.4kN. The theoretical yield capacity of 28 UFPs was 826kN. The experimental values ranged from 864.5kN to 917.8kN. An overstrength factor of 1.3 was used for strain hardening as suggested by Kelly et al. (1972). The ultimate capacity of the single UFP was expected to be 38.4kN. For 8 UFPs the ultimate capacity was 307.2kN. The experimental ultimate capacity ranged from 278.8kN to 304.5kN. For 28 UFPs the ultimate capacity was 1075.2kN. The experimental values ranged from 999.6kN to 1022.6kN. Main structural properties are listed in Table 3. The experimental data was consistent with the theoretical values. The overstrength factors ranging from 1.1 to 1.3 were obtained from the experimental results. All the specimens were able to achieve the displacement ductility of 3.5 to 4.0 except for specimen 2 which was able to reach the displacement ductility of 7.4 in tension. Performance parameters of the specimens including initial stiffness (K_i), effective stiffness (K_e), residual displacement (RD) and residual stress (RS) were listed in Table 4.

All the three specimens exhibited stable hysteretic behaviours. Figure 6a shows an example of the hysteresis curve. The spikes shown in the curve were caused from the slippage of the M12 bolts. In Test 1 and 2 the overstrength in compression was less than 1.09. In test 3 and 4 the overstrength in compression was 1.02 or less. Comparing to the overstrength in compression of the Buckling Restrained Brace (BRB) which typically ranges from 1.1 to 1.3 (Chou et al., 2012 & Landolfo et al., 2017) the structural behaviours of the MUD in tension and compression were relatively symmetric. However, possible changes can be made to reduce the overstrength in compression in the future design to have symmetric arrangement with half of UFPs facing upwards and the other half of UFPs facing downwards. Also hot rolled UFPs can be used instead of the cold rolled UFPs. The backbone curve and the idealized bilinear response for each specimen were plotted in Figure 6b. The performance of each specimen was consistent and repeatable.

Figure 7 shows the energy dissipating capacity of each specimen per cycle and the cumulative energy dissipation. The amount of energy dissipated per cycle increased as the displacement amplitude increased. The energy dissipating behaviour of the same specimen (e.g. test 1 and test 2) were consistent and repeatable. The more UFPs that were used the more the energy dissipated. The cumulative energy dissipation in test 3 was 3.2 times that in test 2, so did the energy dissipation per cycle. The comparison of the equivalent viscous damping ratio for each test is shown in Figure 8. The equivalent viscous damping ratio increased as the displacement amplitude increased. With the repetition of the 45mm displacement, the damping ratio remained stable. The values of damping ratio in the three tests at 60mm displacement amplitude were 46.3%, 47.5% and 44.4% respectively. An energy-based method was used to obtain the damping ratio, which can be evaluated as the ratio between the energy dissipated per cycle and the potential energy.
Figure 9 a) and b) illustrate the comparison of the capacity degradation and the stiffness degradation between each test respectively. All the specimens performed well without obvious drop in capacity and stiffness during the test. The performance of the same specimen was highly consistent. In Test 2 and 3, minor decrease in capacity was observed in Figure 9 in the last cycle, which may be caused by the damage in the UFP. One UFP was fractured in test 2. The tension capacity dropped by 19kN in total (6.8% reduction in capacity) and the compression capacity dropped by 7.5kN (2.5% reduction in capacity). In test 3 one UFP was broken and two UFPs suffered very minor cracking of the edges. Total decrease in tension capacity was 55kN (5.6% reduction in capacity) and total decrease in compression capacity was 30.5kN (3.0% reduction in capacity).

3.3 Results from test 4

Specimen 4 has been through three times the maximum credible earthquakes and 46 loading cycles at 2% inter-storey drift (at 45mm axial displacement), where a diagonally braced frame with a storey height of 3.0m and a bay length of 3.1m was assumed, and the 45mm axial elongation of the diagonal brace was equivalent to a 62mm lateral displacement in the braced frame. The specimen exhibited a very stable and symmetric hysteresis behaviour (Figure 10a). The yield strength of 918kN in tension and 878kN in compression obtained from the test were slightly higher than the theoretical value of 826kN (Figure 10b). The axial load capacity reduced by 30% only and the test was terminated. A gradual reduction in capacity was also observed which indicates that the MUD brace has a promising ability to prevent sudden failure of the structure (Figure 11a). The effective stiffness remained relatively constant until the last 10 loading cycles where the stiffness started to reduce moderately due to the formation of the fractures in the UFPs (Figure 11b). The sudden drops in capacity and stiffness as shown in Figure 11 were resulted from repeating the loading sequence from 4mm to 60mm. The results also showed that the MUD was able to dissipate energy effectively and maintain its capacity for a large number of cycles beyond the yield point and after the formation of the cracks in the UFPs (Figure 12a, 12b).

4 CONCLUSION

Specimen 1, 2 and 3 sustained 14 additional cycles at 45mm displacement ($1.5\Delta_{bm}$) without suffering strength degradation. They performed significantly better than required by the AISC 341-16. The test results showed that the MUD is able to achieve great robustness. All specimens completed the cyclic testing up to 2.8% story drift. They exhibited stable force-displacement hysteresis and high energy dissipation capacity. The experimental yield strength, maximum tension force and maximum compression force were consistent with the theoretical values. Specimen 4 sustained 66 additional cycles than required by the AISC 341-16 at amplitude ranging from 4mm to 60mm. The strength and stiffness reduced gradually which showed a promising ability to prevent sudden failure of the structure. There was no damage observed in the internal and external member after all the tests. These members can be reused after a major earthquake. This is a great advantage comparing to other brace members such as BRB considering the repair cost and time efficiency. In this research the specimens showed promising performance which gives more confidence for future research. Parametric analysis will be carried out in the next stage, the aim is to optimise the MUD design in order to reduce material use and to develop a replaceable member so that the UFPs can be easily inspected and replaced.

Table 3: Main structural properties of test specimens

	Tension						Compression					
	F_{y_T} (kN)	F_{u_T} (kN)	Φ_{o_T}	Δ_{y_T} (mm)	Δ_{u_T} (mm)	μ_T	F_{y_C} (kN)	F_{u_C} (kN)	Φ_{o_C}	Δ_{y_C} (mm)	Δ_{u_C} (mm)	μ_C
Test 1	252.9	281.2	1.11	16.0	59.5	3.7	262.8	302.1	1.15	16.0	60	3.8
Test 2	216.5	278.8	1.29	8.0	59.5	7.4	265.4	304.5	1.15	16.0	59.5	3.7
Test 3	893.1	999.6	1.12	17.0	59.5	3.5	864.5	1022.6	1.18	17.0	60	3.5
Test 4	917.8	1002.3	1.09	15.0	59.6	4.0	878.5	1022.2	1.16	16.0	60	3.8

Table 4: Main performance parameters of test specimens

	Tension		Compression			
	K_i (kN/mm)	K_e (kN/mm)	K_i (kN/mm)	K_e (kN/mm)	RD (mm)	RS (kN)
Test 1	32.3	4.7	26.8	5.0	36.0	237.0
Test 2	31.2	4.7	25.3	5.1	36.1	229.7
Test 3	83.1	16.7	69.25	17.0	33.2	748.3
Test 4	103.3	16.7	73.5	17.0	32.3	371.5

Note: K_i is the initial stiffness; K_e is the effective stiffness; RD is the residual displacement; RS is the residual stress.

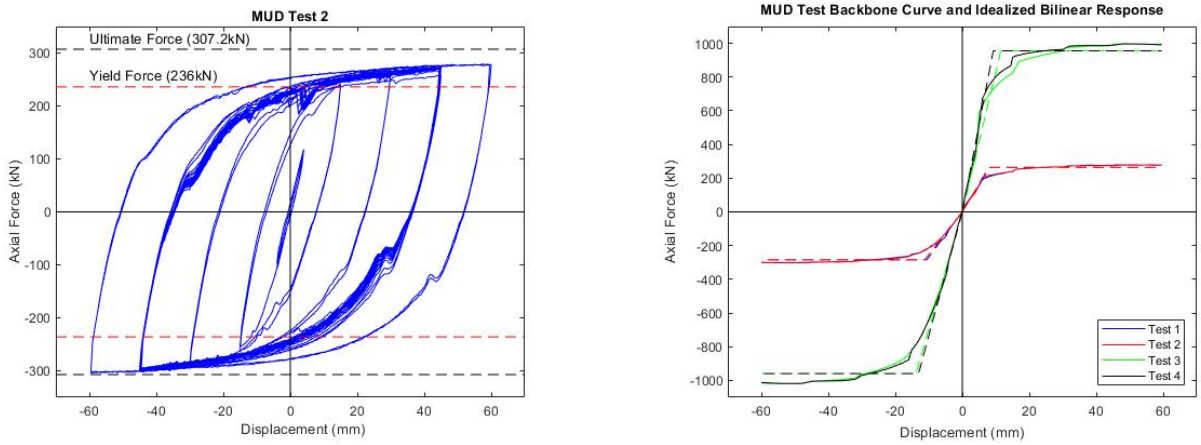

Figure 6: a) Example of experimental hysteresis loop; b) Backbone curve and idealized bilinear response

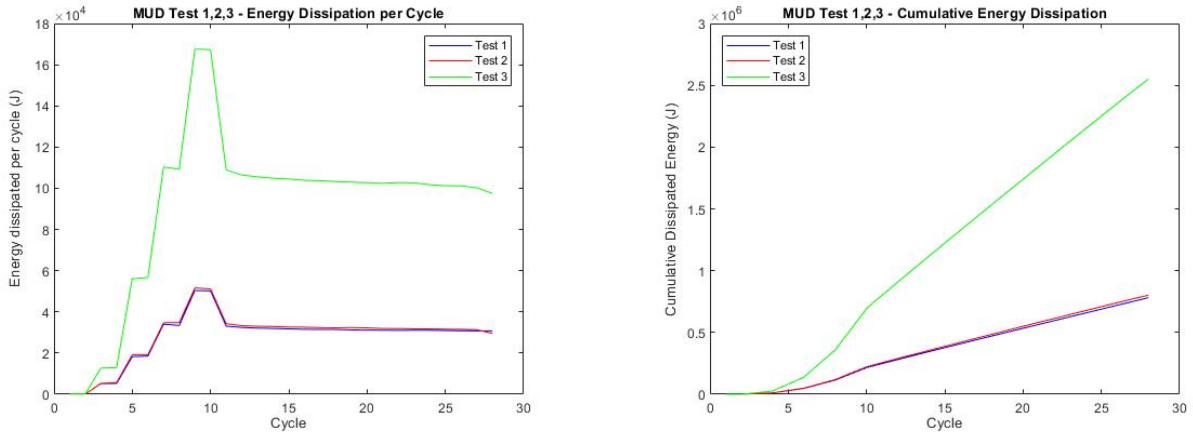

Figure 7: a) Comparison of energy dissipation per cycle; b) Comparison of cumulative energy dissipation

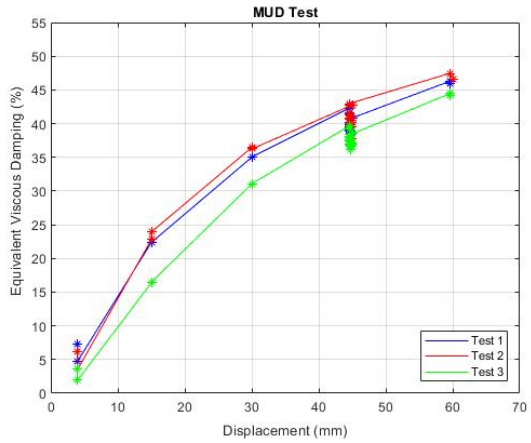

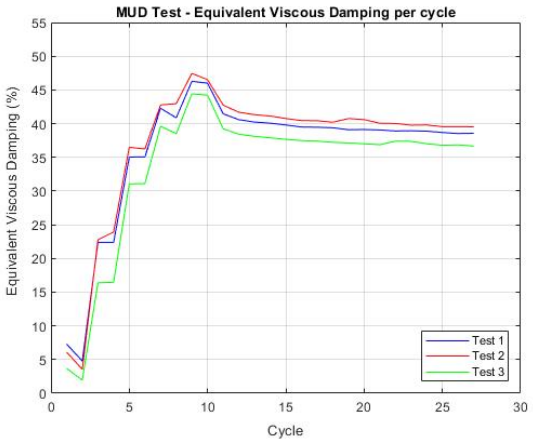

Figure 8: Comparison of equivalent viscous damping

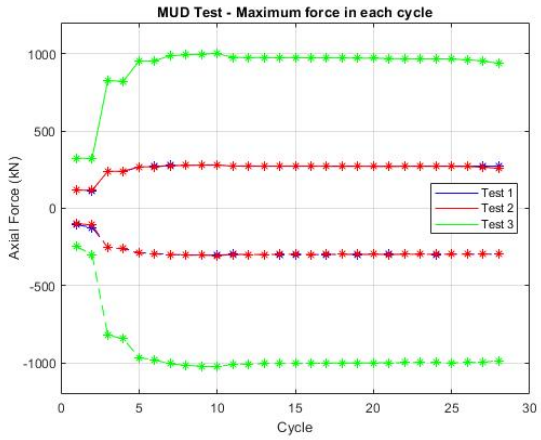

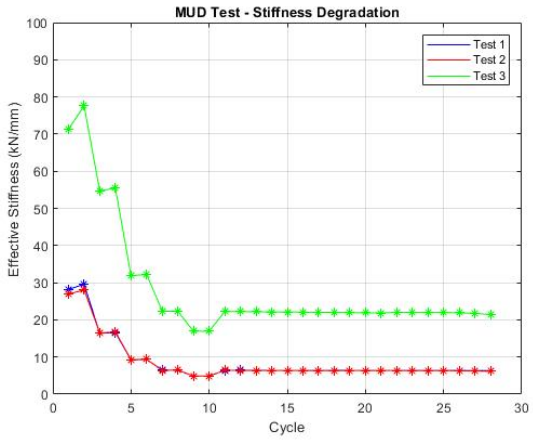

Figure 9: a) Comparison of capacity degradation; b) Comparison of stiffness degradation

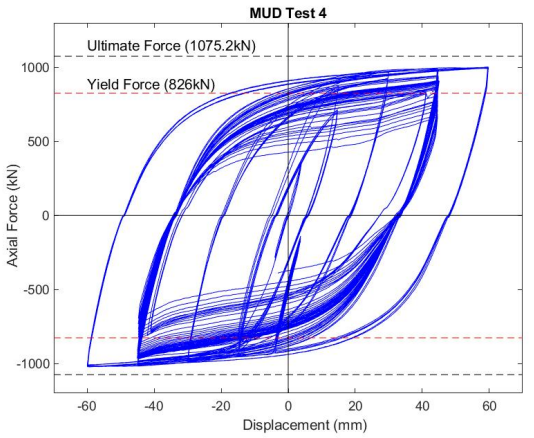

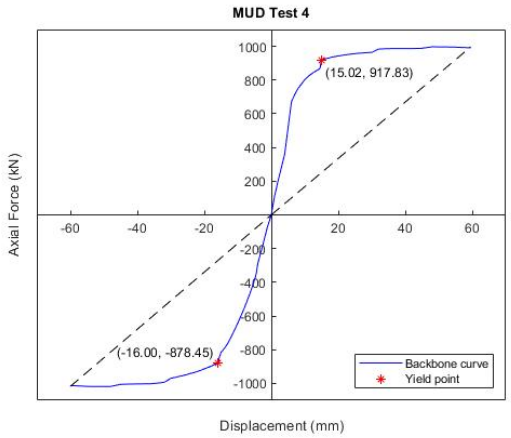

Figure 10: a) Hysteretic curves - test 4; b) Identification of the yield strength - test 4

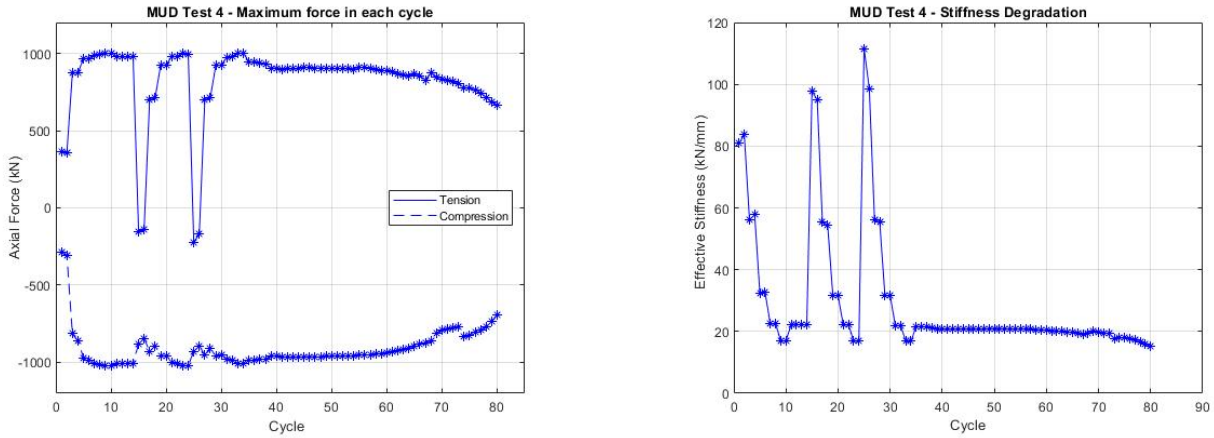

Figure 11: a) Capacity degradation - test 4; b) Stiffness degradation - test 4

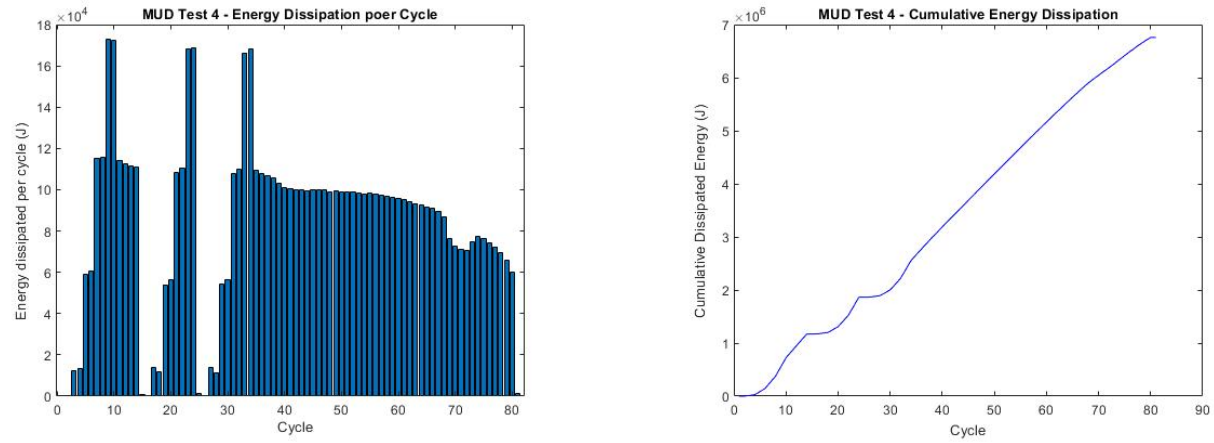

Figure 12: a) Energy dissipation per cycle - test 4; b) Cumulative energy dissipation - test 4

5 ACKNOWLEDGEMENT

The authors greatly acknowledge the support by 2.2 GForce Limited.

REFERENCES

ANSI/AISC 341-16. (2016). *Seismic Provisions for Structural Steel Buildings.* Chicago: American Institute of Steel Construction.

Buchanan, A., Bull, D., Dhakal, R. P., MacRae, G., Palermo, A. and Pampanin, S. (2011). *Base Isolation and Damage-Resistant Technologies for Improved Seismic Performance of Buildings.* Christchurch, New Zealand: Canterbury Earthquakes Royal Commission.

Baird, A., Smith, T., Palermo, A., Pampanin, S. (2014). Experimental and Numerical Study of U-shape Flexural Plate (UFP) Dissipaters. *2014 NZSEE Conference.*

Canterbury Earthquakes Royal Commission. (2012). *Final Report – Volume 3: Low-Damage Building Technologies.* Christchurch, New Zealand: Canterbury Earthquakes Royal Commission.

Chou, C., Liu, J., Pham, D. (2012). Steel buckling-restrained braced frames with single and dual corner gusset connections: seismic tests and analyses. *Earthquake Engineering & Structural Dynamics*, 2012 (41), 1137-1156.

Jiao, Y., Kishiki, S., Yamada, S., Ene, D., Konishi, Y., Hoashi, Y., Terashima, M. (2015). Low Cyclic Fatigue and Hysteretic Behaviour of U-shaped Steel Dampers for Seismically Isolated Buildings under Dynamic Cyclic Loadings. *Earthquake Engineering & Structural Dynamics, 2015 (44), 1523-1538.*

Keats, G., Palermo, A., Mashal, M. M., Energy Dissipation Device. 61/149, 199; 2015.

Keats, G., Palermo, A., Mashal, M. M., Energy Dissipation Device. PCT/NZ2016/050061; 2016.

Kelly, J. M., Skinner, R. I., Heine, A. J. (1972). Mechanisms of Energy Absorption in Special Devices for Use in Earthquake Resistant Structures. *Bulletin of N.Z. Society for Earthquake Engineering,* Vol. 5 (No. 3): 287-296.

Landolfo, R., Mazzolani, F., Dubina, D., da Silva, L. S., D' Aniello, M. (2017). *Design of Steel Structures for Buildings in Seismic Areas.* Brussels: ECCS – European Convention for Constructional Steelwork.

Mashal, M., Palermo, A., Keats, G. (2019), Innovative metallic dissipaters for earthquake protection of structural and non-structural components. *Soil Dynamics and Earthquake Engineering,* 116 (2019), 31-42.